

1 **Climatology, variability and trends in United States**
2 **vapor pressure deficit, an important fire-related**
3 **meteorological quantity**

4 RICHARD SEAGER*

Lamont Doherty Earth Observatory of Columbia University, Palisades, New York

5 ALLISON HOOKS

Columbia College, Columbia University, New York, New York

6 A. PARK WILLIAMS

Lamont Doherty Earth Observatory of Columbia University, Palisades, New York

7 BENJAMIN COOK

NASA Goddard Institute for Space Studies, New York, New York

8 JENNIFER NAKAMURA AND NAOMI HENDERSON

Lamont Doherty Earth Observatory of Columbia University, Palisades, New York

* *Corresponding author address:* Richard Seager, Lamont Doherty Earth Observatory of Columbia University, 61 Route 9W., Palisades, NY 10964. Email: seager@ldeo.columbia.edu, Tel: 845-365-8743, FAX: 845-365-8736

Submitted to *Journal of Applied Meteorology and Climatology* July 2014. LDEO Contribution Number xxxx.

ABSTRACT

10 Unlike the commonly used relative humidity, vapor pressure deficit (*VPD*), is an absolute
11 measure of the difference between the water vapor content of the air and its saturation value
12 and an accurate metric of the ability of the atmosphere to extract moisture from the land
13 surface. *VPD* has been shown to be closely related to variability in burned forest area in
14 the western United States. Here the climatology, variability and trends in *VPD* across the
15 U.S. are presented. *VPD* reaches its climatological maximum in summer in the interior
16 southwest U.S. due to both high temperatures and low vapor pressure under the influence
17 of the northerly, subsiding eastern flank of the Pacific subtropical anticyclone. Maxima of
18 variance of *VPD* are in the southwest and southern Plains in spring and summer and are to
19 a large extent driven by temperature variance but vapor pressure variance is also important
20 in the southwest. La Niña-induced circulation anomalies cause subsiding, northerly flow
21 that drive down actual vapor pressure and increase saturation vapor pressure in fall through
22 spring. High spring and summer *VPD* can also be caused by reduced precipitation in
23 preceding months, as measured by Bowen ratio anomalies. A case study of 2002 leading
24 up to the Rodeo-Chediski, AZ, and Hayman, CO. fires shows very high *VPD* caused by
25 antecedent surface drying and subsidence warming and drying of the atmosphere. *VPD* has
26 increased in the southwest U.S. since 1961, driven by warming and a drop in actual vapor
27 pressure, but decreased in the northern Plains and midwest, driven by an increase in actual
28 vapor pressure.

1. Introduction

In, for the field of meteorology, an unusually passionate polemic, Anderson (1936) argues for measuring and reporting the water vapor content of the atmosphere relative to saturation in terms of vapor pressure deficit (VPD) rather than relative humidity (RH). VPD is the difference between the saturation vapor content of air at temperature T_a , $e_s(T_a)$, and its actual vapor pressure, e_a , viz:

$$VPD = e_s(T_a) - e_a, \tag{1}$$

whereas RH is given by their ratio expressed in percent form, viz:

$$RH = 100 \times \frac{e_a}{e_s(T_a)}. \tag{2}$$

Anderson (1936) points out that RH is not an absolute measure but merely a ratio of two known quantities expressed as a percentage. In contrast VPD gives an absolute measure of the atmospheric moisture state independent of temperature. For example, the same VPD above a surface that is not water-limited and for a given wind speed and atmospheric stability, leads to the same rate of evaporation, regardless of temperature. Expressing RH and VPD in terms of each other we get:

$$RH = 100(1 - VPD/e_s(T_a)), \tag{3}$$

$$VPD = e_s(T_a)(1 - RH/100). \tag{4}$$

In these relations we see the basic problem with RH . For any given RH the VPD varies exponentially because of the Clausius-Clapeyron dependency of $e_s(T_a)$ on T_a . That is, at very low temperatures a given RH will correspond to a very small VPD while at high temperatures the same RH will correspond to a very high VPD . Similarly a given VPD will correspond to a much higher RH at high temperatures than at lower temperatures. The point of Anderson (1936) was that the water balance stress placed upon an organism is determined by the VPD and not the RH . Despite his arguments VPD has not exactly

53 caught on. The daily weather forecasts still routinely report *RH* but never *VPD* and
54 meteorologists and the public alike are far more familiar with *RH* reports, often mentally
55 factoring in the temperature dependence when considering the implications.

56 Despite the lack of popularity of *VPD* it deserves a new lease on life. In two recent papers
57 Williams et al. (2014b,a) show that *VPD* is the meteorological variable that best correlates
58 with burned area for forest fires in the U.S. southwest over past decades. Forest fire is an
59 every year concern in the southwest U.S. Though fire is a naturally occurring phenomenon
60 to which forest ecosystems, including fauna and flora, are adjusted and, in some cases, even
61 dependent upon, it poses considerable problems for society. First is of course the protection
62 of life which has become ever more difficult as the population of the southwest has expanded
63 and more and more people are living at the 'urban-forest interface' (Pyne 2009). After this,
64 damage to property is a concern. Further, and quite fundamentally, the lands of western
65 North America are now all, to a greater or lesser extent, managed by people and, very often,
66 even if indirectly, by the Federal government. Dealing with fire is one of the key problems of
67 land management; how to manage a process that is at the same time natural and essential
68 and tremendously damaging? Now that western forests are experiencing drought and heat
69 stress combined with outbreaks of bark beetles and unprecedented areas of burns, stresses
70 that are expected to only get worse as human-induced climate change advances (Allen
71 et al. 2010; Bentz et al. 2010; Williams et al. 2013), fire-management is ever more important
72 (Stephens et al. 2013). Hence it is imperative to better understand the processes that control
73 fire.

74 Many prior studies have sought relationships between climate and wildfire (e.g. West-
75 erling et al. (2003, 2006); Westerling and Bryant (2008); Littell et al. (2009); Abatzoglou
76 and Kolden (2013); Riley et al. (2013)). In regard to links between climate and forest fire
77 incidence *VPD* explains more variance than precipitation, various drought indices and tem-
78 perature individually can (Williams et al. 2014b; Sedano and Randerson 2014)). This is of
79 course a confirmation of Anderson (1936)'s plea for the ecological relevance of *VPD*. It is
80 not surprising that *VPD* is more successful in explaining burned forest fire area than other
81 variables are. It is essentially a measure of the ability of the atmosphere to extract moisture
82 from the surface vegetation thus reflecting variations in the moisture content and flammabil-

83 ity of forests. It is more explanatory in this regard than RH because it accounts for the fact
84 that it is the combination of low RH and high temperature that creates the most fire-prone
85 conditions. VPD is also more explanatory than temperature (e.g. Westerling et al. (2006))
86 since it reflects the nonlinear dependence of e_s on temperature and also measures the actual
87 moisture content of the air, with the combination of high e_s and low e_a creating the most
88 fire prone conditions. Of course VPD only indirectly measure the antecedent soil moisture
89 conditions which also influence the current moisture content of vegetation. Hence it might
90 be expected that preceding precipitation, or an index of current drought severity (such as
91 Palmer Drought Severity Index that factors in prior precipitation and estimates of evap-
92 otranspiration), would offer additional explanatory power over VPD alone. Consistently,
93 Williams et al. (2014b,a) found a combination of current VPD and prior year precipitation
94 offered the best explanation of burned forest area.

95 Given the demonstrated importance of VPD to at least one topic of great ecological
96 and social importance, it seems worthwhile to explore better the basic spatial and temporal
97 variations of VPD across North America in terms of seasonal cycle, geographic variation,
98 interannual variability and long term trends. To our knowledge no such study has been
99 conducted. Gaffen and Ross (1999) did conduct a study of climatology and trends of spe-
100 cific and relative humidity across the U.S. Their maps of daytime RH show, in winter, high
101 values along the west coast and in the southeast and low values in the northeast and, in
102 summer, a striking west-east lower-higher contrast. Interesting though these maps are, it is
103 almost automatic to ask what controls these temporal and spatial distributions - tempera-
104 ture, specific humidity or both? - and how do they relate to the difference between actual
105 and saturation water vapor content?

106 The current study is motivated both by the desire to develop a better understanding of
107 the controls on moisture undersaturation in the atmosphere and also the need to improve
108 understanding of the outbreak and spread of forest fires. As such, after providing a cross-U.S.
109 analysis of the climatology and variability of VPD we will examine the atmosphere-ocean-
110 land causes of VPD variability in the southwest, as well as the long terms trends in VPD .
111 We will also provide a case study of the VPD anomalies, and their causes, leading up to
112 June 2002 when two major southwest fires (the Rodeo-Chedeski and Hayman fires) occurred.

2. Data and Methods

High quality, spatially and temporally extensive humidity data are hard to come by in general. Here we use the PRISM data set developed by the PRISM Climate Group at Oregon State University, details of which can be found at <http://www.prism.oregonstate.edu> and in Daly et al. (2000), and which was obtained from the International Research Institute for Climate and Society as <http://iridl.ldeo.columbia.edu/SOURCES/.OSU/.PRISM/>. Because of data availability we limit ourselves to the 1961 to 2012 period (see Williams et al. (2014b,a) for this rationale). The PRISM data provides monthly means of maximum (T_{max}) and minimum (T_{min}) daily temperature and dew point temperature (T_d). The mean monthly air temperature is approximated as $T_a = (T_{max} + T_{min})/2$ and $e_s(T_a)$ and e_a are calculated from:

$$e_s(T_a) = e_{s0} \exp[17.67(T_a - T_0)/(T_a - T_0 + 243.5)], \quad (5)$$

$$e_a = e_{s0} \exp[17.67(T_d - T_0)/(T_d - T_0 + 243.5)], \quad (6)$$

where T_a and T_d are in Kelvin and $T_0 = 273.15K$. We are aware that because of the nonlinear dependence of e_s on T_a any averaging of temperatures in space and time introduces errors in the sense of underestimating e_s . Williams et al. (2014b,a) in their study of the southwest U.S. did account for this by using some statistical relationships between daily and monthly temperature data. Here we do not do this and instead simply compute e_s from averaged temperature. It is considered, after evaluation, that the approximation introduces an acceptable degree of error. For geopotential heights and vertical velocities we use the National Centers for Environmental Prediction-National Center for Atmospheric Research (NCEP-NCAR) Reanalysis (Kalnay et al. 1996; Kistler et al. 2001). The NCEP-NCAR Reanalysis was chosen as the only Reanalysis that assimilates all available information that extends back before 1979 and hence overlaps the PRISM precipitation data. For surface sensible and latent heat fluxes, used to compute Bowen ratio, we used data from the Global Land Data Assimilation System (GLDAS) 2.0 available at http://disc.sci.gsfc.nasa.gov/gesNews/gldas_2_data_release. GLDAS uses a land surface model forced by observed meteorological conditions to estimate the land surface hydrology and surface fluxes of water

140 and energy (Rodell et al. 2004; Sheffield and Wood 2006). All analyses cover the 1961 to
141 2012 period and anomalies, when used, are with respect to a climatology over this period.

142 **3. Climatology of vapor pressure deficit across the U.S.**

143 Figure 1 shows the VPD , e_s and e_a for the four seasons of October to December (OND),
144 January to March (JFM), April to June (AMJ) and July to September (JAS), which cor-
145 respond to the hydrological year and which we shall refer to as fall, spring, summer and
146 fall. The VPD is lowest in the winter season, that is, the air is closest to saturation at this
147 time. This is partially caused by the low e_s , following on the coldest temperatures of the
148 year, which places an upper bound on how large VPD can be. A vast area of western North
149 America and northern central and eastern North America has e_s below 5mb in the winter.
150 The VPD pattern is largely zonal in winter because the warmer west coast areas with higher
151 e_s are also areas of higher e_a . The coastal eastern regions have less of a maritime climate
152 and a more continental climate because of the prevailing westerlies and VPD , e_s and e_a here
153 are contiguous with the interior U.S. to the west.

154 By spring the VPD has climbed above 5mb across most of the U.S. except for parts of
155 the northwest, some areas south of the Great Lakes and northern Maine. What is striking is
156 the area of 20–30mb VPD in the interior southwest U.S. This is driven by a sharp rise in e_s .
157 However, e_s rises by just as much across the southern central and southeast U.S.. However,
158 in these regions this does not translate into a similar rise in VPD because e_a also rises to
159 keep track while it does not in the interior southwest. These differences are, in turn, related
160 to the development of the Atlantic subtropical high and moisture convergence in southerly
161 flow over the southern U.S. (e.g. Seager et al. (2003b)) whereas moisture flow into the
162 interior southwest awaits the reach of the North American Monsoon (Adams and Comrie
163 1997). The switch from winter with northerly flow to spring with southerly flow, associated
164 with development of the Atlantic subtropical high, is evident in the rise of e_a across the U.S.
165 from the Plains to the Atlantic coast.

166 In going from spring to summer VPD increases modestly over the eastern U.S., especially
167 in the northern region but climbs strongly in the southwest. The highest monthly mean

168 values that ever occur in the U.S. (close to 50mb) occur in summer in southeastern California,
169 southern Nevada and southwestern Arizona. This is related to high temperatures driving
170 high e_s and outstripping the increase in e_a . Texas is the other region of widespread high
171 VPD which arises from very high e_s and relatively low e_a away from the Gulf coast. High e_a
172 across the remainder of the southern U.S. and the southeast balances high e_s and keeps VPD
173 relatively low. The northwest, north central and northeastern U.S. have their maximum
174 VPD in summer as e_a fails to keep up with the highest values of e_s driven by the warmest
175 temperatures of the year. In fall all quantities are well on their way, after summer, to
176 re-establishing their winter states.

177 4. Interannual variability of VPD across the U.S.

178 While the climatology of VPD is interesting, ecosystems are presumably largely evolved
179 to deal with this. They will also be able to adapt, to some extent, to year-to-year variabil-
180 ity. However extreme high VPD years are expected to exert considerable water stress on
181 vegetation risking disease, fire and mortality. Hence we next turn to examine the variability
182 of VPD and its causes over the post 1961 period. To do this we computed the variance of
183 VPD , e_s and e_a for each month and then averaged these monthly variances to form seasonal
184 mean variances which are shown in Figure 2.

185 In no season is the VPD variance simply proportional to the VPD climatology. In the
186 fall and winter the VPD variance has a southwest maximum, northeast minimum pattern
187 with lines of equal variance oriented in a roughly northwest to southeast manner. This is in
188 contrast to the more zonal pattern of the VPD climatology. This VPD variance pattern is
189 quite distinct from that of the e_s and e_a variances which are maximum over the southeastern
190 U.S. Since these do not translate into a VPD variance maximum it must be because they
191 vary together, i.e. $e'_s \approx e'_a$, $(e_s - e_a)' \approx 0$. One reason for this is that in these seasons transient
192 eddies dominate the moisture convergence into the southeastern and eastern U.S. (Seager
193 et al. 2014b). The eddies act to diffuse temperature and moisture such that, in southerly flow
194 they will both warm, increasing e_s , and moisten, increasing e_a , and vice versa for northerly
195 flow, minimizing the change in VPD . In contrast, in the southwest the e_s variance is large

196 and must not be compensated for by e_a variance. These comparisons make clear that, in
 197 general, the VPD variance can not be explained as being purely temperature driven with,
 198 for example, e_s varying and the VPD variations simple related to this according to fixed
 199 RH .

200 In the spring the southwest region of climatological high VPD is also a region of high
 201 VPD variance and this seems driven by high e_s variance, i.e. by temperature variance, while
 202 the e_a variance is quite low. There is also a central U.S. maximum of VPD variance that
 203 stretches from Texas north to Canada which arises from a maximum of e_s , i.e. temperature,
 204 variance. In the summer many of the features of VPD and e_s variances seen in spring remain
 205 but are amplified. Maximum VPD variance occurs in the Mojave, Sonora and Chihuahua
 206 Desert portions of the southwest U.S. These are all regions of high e_s variance. In summer
 207 an e_a variance maximum develops in southeast California and southwest Arizona which is
 208 likely due to variance of moisture convergence in the North American Monsoon.

209 The regions of low spring and summer e_s variance in the interior west, which translate
 210 into lower VPD variance are related to high topography where the climatological e_s and
 211 e_a are lower than in lower-lying surrounding areas (Figure 1). This can be understood as
 212 follows. The e_s variance for a given month is given by:

213

$$\sigma_{e_s} = \frac{1}{N} \sum_{n=1}^N e_{s,n}'^2, \quad (7)$$

214 where n indicates year and N is the total number of years. e_s' can be linearized as:

215

$$e_s' \approx \left. \frac{de_s}{dT} \right|_{\overline{T_a}} T_a', \quad (8)$$

216 that is, the gradient of e_s with respect to T evaluated at the climatological mean air tem-
 217 perature, $\overline{T_a}$, multiplied by the air temperature anomaly, T_a' . Substituting Eq. 8 into Eq. 7
 218 we get:

219

$$\sigma_{e_s} = \frac{1}{N} \sum_{n=1}^N \left(\left. \frac{de_s}{dT} \right|_{\overline{T_a}} T_a' \right)^2. \quad (9)$$

220 Since de_s/dT increases with T , the same temperature variance will give lower e_s variance
 221 at lower climatological mean temperatures. When e_s variance is estimated with Eq. 9 (not

222 shown) it is clear that this effect, in combination with lower temperature variance at colder
223 temperatures, explains the low e_s and VPD variance at higher elevations in western North
224 America.

225 The clear and expected increase of variance of vapor pressure quantities with the mean
226 values suggest that normalized variance may be a more informative measure. Hence Figure
227 3 shows the variances normalized by their climatological values and expressed as a fraction.
228 In this case large values show that the variance is unusually large in comparison to its
229 climatological value while small values show the opposite. The southwest desert maximum
230 of VPD variance does not appear in the maps of normalized variance. Instead the normalized
231 variance of VPD emphasizes the southern Plains in spring, the entire Plains in summer and
232 many southwestern areas in California, Arizona, New Mexico, Colorado and Utah. Also
233 some areas of relatively low absolute VPD variance in the Pacific northwest states appear
234 as high areas of relative variance. The normalized variances of e_a are also different to those of
235 absolute e_a . While the latter track the climatological e_a , the former shows the southwest areas
236 of high VPD variances to be ones of high e_a variance. Looked at in this way, it appears that
237 high VPD variance in regions of the southwest does not just arise from high temperature,
238 e_s , and e_s variance but also from relatively high e_a variance. This is suggestive of a potential
239 role for driving of atmospheric humidity variability by locally strong atmospheric circulation
240 variability, that is, a role for atmospheric dynamics as well as thermodynamics.

241 Figure 4 shows all areas that have burned across the western U.S. from 1984 to 2011
242 based on the Monitoring Trends in Burn Severity data (www.mtbs.gov, Eidenshink et al.
243 (2007)). This can be qualitatively be compared with the climatology and variance figures
244 above. Clearly the area in the deep southwest at the California-Arizona border that has high
245 climatological and absolute (but not normalized) variance of VPD is not an area of frequent
246 and widespread burns which is probably because of the lack of fuel. Burns are common
247 and widespread in a swath of land across southern and central Arizona and New Mexico,
248 western Texas, Oklahoma and eastern Kansas, extend north through the Plains, Nebraska
249 and Montana linking to an area of widespread burns in Idaho, eastern Washington and
250 Oregon and northern Nevada. Other areas of widespread burns are the coastal and Sierra
251 Nevada ranges of California. This bears some similarity to the maps of spring and summer

252 normalized *VPD* variance. A perfect match would not be expected given the control that
253 fuel availability, for example, and other factors will exert on burned area (Swetnam and
254 Betancourt 1998; Westerling et al. 2002, 2003; Littell et al. 2009; Abatzoglou and Kolden
255 2013). So, for example, the tremendous maximum of variance in Texas and the southern
256 to central Plains does not translate into a similarly impressive maximum in burned area.
257 That may be because this is an area of grasslands rather than forest but, nonetheless, this
258 is a local maximum of burned area. Similarly the general donut of burn areas in the Plains,
259 northern states, California and the southwest, ringing a burn area donut hole in the interior
260 west, is also seen in *VPD* variance. Much of this donut hole is very high altitude with
261 low climatological and variance of temperature or high desert with little vegetation to burn.
262 Another notable feature is that, despite the relatively low climatology and variance of *VPD*
263 in the northwestern states, the relatively high normalized *VPD* variance matches the high
264 burned area in this region. The exception is the coastal northwest where low burned area
265 corresponds to low normalized *VPD* variance. All these relations make clear the importance
266 to fire incidence and spread of *VPD* and how its variance compares to the mean conditions.
267 Areas with lower mean *VPD* but relatively high variance seem to be able to have greater
268 burned area than those with higher *VPD* and relatively lower variance.

269 **5. Relationship of *VPD* variability in the southwest U.S.** 270 **to SST and circulation variability**

271 As shown in Williams et al. (2014b,a), interannual *VPD* variability is the best predictor
272 of burned forest area in the southwest U.S. The analysis above has shown that *VPD* vari-
273 ability is largest in the southwest U.S. at the California-Arizona border. However this is a
274 very arid region, with high climatological *VPD*, and not one with extensive fire occurrence
275 due to the absence of extensive vegetation. Fire occurrence is more common in regions of
276 lower climatological *VPD* that are less arid and can sustain vegetation that is nonetheless
277 susceptible to burning. We have already shown that *VPD* variability is large in these inter-
278 mediate aridity regions in the spring and summer seasons critical for fires and that this is

279 influenced strongly by e_s variability but also by e_a variability. But what controls VPD , e_s
280 and e_a variability?

281 To look at this we examine relations between VPD , e_s and e_a and atmospheric circulation,
282 as measured by the 700mb geopotential height, and sea surface temperature (SST) variability.
283 We focus in on the region of high fire occurrence identified by Williams et al. (2014b,a). This
284 southwest area lies to the east of the region of very high VPD climatology and variance
285 at the California-Arizona border and includes the parts of Arizona, New Mexico, Texas,
286 Oklahoma, Colorado and Utah bounded by $28.5^\circ N$ and $38^\circ N$ and to the west of $100^\circ W$.
287 The 700mb level is chosen since this more closely corresponds to the level in the atmosphere
288 where significant moisture transport occurs. Results are shown in Figure 5. In fall, winter
289 and spring high VPD in the southwest correlates with local high pressure. In fall this is
290 part of a zonal wave pattern and in winter and spring it is part of a general mid-latitude
291 ridge that extends across the Pacific, North America and the Atlantic. High VPD is also
292 correlated with cool tropical Pacific SSTs in winter and spring and, to a lesser extent, in
293 fall. The circulation patterns are what is expected given the La Niña SST pattern (Seager
294 et al. 2003a, 2005, 2014a). These relations make clear that high VPD in the southwest is
295 promoted by La Niña conditions. This relation breaks down in the summer which is expected
296 given the general weakness of tropical-mid-latitude teleconnections in the summer (Kumar
297 and Hoerling 1998).

298 High e_s is also correlated with high geopotential heights and La Niña SST conditions and
299 the patterns of each are quite similar to those for the VPD correlations. This indicates that
300 high VPD anomalies are being driven, in large part, by an increase in temperature causing
301 high e_s . The correlations with e_a are opposite in fall and winter: that is, low e_a , which would
302 contribute to high VPD , also arises from La Niña conditions. The La Niña connection to
303 low e_a is also clear in the spring though the associated height anomaly pattern is different to
304 that for the VPD and e_s correlations. The summer e_a correlation, as expected, does not have
305 a feature in the tropical Pacific and the circulation anomaly indicates high e_a corresponding
306 to low pressure off Baja California and high pressure over the Rocky Mountains.

307 These relations are fairly easy to explain. During La Niña conditions in the fall, winter
308 and spring high pressure develops over the southwest which favors subsidence beneath caus-

309 ing both high temperatures and high e_s , via warming due to compression, and low e_a due
310 to the subsidence of dry air. Both effects drive the VPD to be high. In summer, when the
311 connection to the tropical oceans is weak, high VPD and e_s in the southwest are still favored
312 by local high pressure (and, presumably, subsidence warming) while low e_a appears to be
313 favored by flow anomalies from the north and west, which makes sense since the moisture
314 sources for the southwest lie to the south over the Gulfs of California and Mexico.

315 **6. Relationship of variability of VPD to land surface** 316 **conditions**

317 While atmospheric circulation anomalies are expected to be able to influence VPD in-
318 stantaneously via subsidence of warm, dry air, it is also expected that previous reductions
319 in precipitation could dry out the soil and lead to an increase in VPD . As the soil dries
320 out incoming solar radiation needs to be increasingly balanced by sensible and long wave
321 radiative heat loss, and less by evapotranspiration, and this requires an increase in surface
322 temperature at the same time as less moisture flux from the surface to the atmosphere, both
323 effects increasing VPD . One measure of soil dryness is the Bowen ration, $B = SH/LH$,
324 where SH is surface sensible heat flux and LH is surface latent heat flux.

325 The previous section showed that VPD increases as atmospheric circulation anomalies
326 cause warming and/or drying. In the absence of a surface moisture anomaly, subsidence
327 warming and drying would be expected to increase LH and reduce SH , surface flux changes
328 that would offset the circulation-induced changes in VPD . This would cause a reduction in
329 the Bowen ratio to accompany the increase in VPD .

330 Figure 6 shows the correlation across North America between seasonal VPD and Bowen
331 ratio. In the southwest and coastal western North America, the Bowen ratio increases with
332 VPD throughout the year. There are negative correlations across the central northern U.S.
333 in fall and most of the central and eastern U.S. in spring. The strongest positive correlations
334 are in the interior West and the Gulf Coast in summer.

335 The cause of these correlations can be understood in terms of the correlation of Bowen

336 ratio with e_s and e_a also shown in Figure 6. The correlation between Bowen ratio and e_a is
337 simple and essentially always negative (except for Pennsylvania, New York and New England
338 in summer). That is as latent heat flux goes up, and Bowen ratio drops, the atmospheric
339 water vapor rises. This suggests the atmospheric vapor pressure responding to changes
340 in evapotranspiration. The relation of Bowen ratio with e_s is more spatially variable. In
341 the central and southern parts of the West Bowen ratio tends to rise as temperature rises
342 while in the central to eastern U.S. and the northwest the Bowen ratio tends to decrease as
343 temperature rises. In winter across most of the U.S. the Bowen ratio tends to decrease as
344 e_s , i.e. temperature, rises.

345 Away from the southwest, the winter relations between Bowen ratio and e_s and e_a can be
346 understood in terms of atmospheric driving. During this season of low evapotranspiration
347 and high surface moisture availability, a warm anomaly (of whatever origin) will cause an
348 increase in e_s , an increase in latent heat flux, a drop in the Bowen ratio, and an increase in
349 e_a . The east-west correlation contrast in summer probably reflects the east-west high-low
350 precipitation/dryness contrast. That is, the eastern half receives considerable precipitation
351 in summer and generally has ample surface moisture supply while the west receives little
352 summer precipitation and the surface dries in summer. As such, warm temperature anomalies
353 can drive higher latent heat flux and lower Bowen ratio during summer in the eastern half of
354 the country. In contrast, across the west throughout the year, moisture is in shorter supply
355 and drying (due for example to a precipitation reduction) can cause a reduction in latent
356 heat flux and both an increase in Bowen ratio and warming as sensible and long wave heat
357 flux rise to balance incoming solar radiation while latent heat flux is reducing. The Bowen
358 ratio-temperature and e_s correlations are, therefore, driven by the atmosphere in the east
359 and by the land surface in the west.

360 The correlation between VPD and Bowen ratio combines the influences of the correlations
361 of Bowen ratio with e_s and e_a . Over the west, in winter, an increase in latent heat flux drives
362 a drop in Bowen ratio, an increase in e_a and drop in VPD . Further east in winter the Bowen
363 ratio and VPD are less correlated while in spring there are areas around the Ohio River
364 valley of negative correlation. This can be explained if a warm anomaly increases latent heat
365 flux and decreases the Bowen ratio and at the same time causes e_s to rise by more than e_a

366 thus increasing the VPD . In the summer, by contrast, VPD and Bowen ratio are positively
 367 correlated essentially everywhere but this is for different reasons in the central to eastern
 368 U.S. and the west because of the opposite sign correlations between e_s and Bowen ratio. In
 369 the moist central to eastern U.S., an increase in surface moisture (say, due to an increase in
 370 precipitation) can cause an increase in latent heat flux and a drop in Bowen ratio but an
 371 increase in e_a and a drop in VPD . The positive VPD - Bowen ratio relation is, however,
 372 much stronger in the dry west. Here a decrease in surface moisture (say, due to a decrease
 373 in precipitation) causes a decrease in latent heat flux and an increase in Bowen ratio but
 374 also an increase in surface temperature and e_s (as less of the incoming solar is balanced by
 375 latent heat flux) and a decrease in e_a and, hence, an increase in VPD .

376 Hence it might be expected that VPD will rise following a period of reduced precipitation
 377 that dries the surface. In contrast changes in atmospheric circulation that cause warming
 378 and/or drying of surface air will near instantaneously cause an increase in VPD . Thus the
 379 land surface and atmospheric circulation mechanisms of altering VPD can work on different
 380 timescales with the former offering potentially longer term predictability.

381 **7. Relation of Southwest and Colorado region VPD to** 382 **the combined effects of land surface and atmospheric** 383 **conditions**

384 To illustrate the effects of land surface and atmospheric conditions we conducted a mul-
 385 tiple linear regression of VPD , Bowen ratio and 700mb geopotential height all averaged over
 386 the Southwest box and a Colorado box ($109^\circ - 101^\circ W, 37^\circ - 41^\circ N$). The Colorado region was
 387 chosen as it encompasses the area of the 2002 Hayman fire discussed below. First we used
 388 linear regression to determine the relation between VPD and Bowen ratio, B , as follows:

$$389 \quad VPD(t) = VPD_B(t) + \epsilon(t) = aB(t) + c + \epsilon(t) \quad (10)$$

390 where $VPD_B(t)$ is the VPD reconstructed on the basis of B alone and ϵ is the unexplained
 391 residual. We then performed a multiple regression between VPD , B and the 700mb geopo-

392 tential height H , as follows:

393

$$VPD(t) = VPD_{BH}(t) + \epsilon'(t) = a'B(t) + b'H(t) + c' + \epsilon'(t) \quad (11)$$

394 where $VPD_{BH}(t)$ is the VPD reconstructed on the basis of B and H , the values of a' and a
395 and c' and c need not be the same and ϵ' is the residual unexplained by the multiple regression.
396 The time series of AMJ seasonal means of VPD_B , VPD_{BH} and the actual AMJ VPD are
397 shown in Figure 7 for the Southwest and Colorado area averages. The reconstructions of
398 VPD based on Bowen ratio alone are not very accurate but the reconstructions based on
399 Bowen ratio (the land surface influence that builds in prior precipitation) and geopotential
400 height (the contemporary atmospheric circulation influence) are reasonably accurate. Bowen
401 ratio and geopotential height together explain 70% and 59% of the variance of AMJ seasonal
402 means of VPD in the southwest and Colorado regions, respectively. Not shown here, but
403 the explained variances were only slightly weaker for summer JAS seasonal means. We are
404 not proposing that such a simple model be used as a potential means for predicting VPD
405 in early fire season but simply wish to better illustrate the land surface and atmosphere
406 controls on VPD . It is quite likely that a more extensive search for predictor variables will
407 lead to better relations than shown here.

408 8. Trends in VPD across the U.S.

409 Next we consider whether there are long term trends in VPD and its contributors.
410 Trends are evaluated via a straightforward least squares regression of seasonal mean VPD ,
411 e_s and e_a for the 1961 to 2012 period and results are shown in Figure 8. Trends in e_s
412 are overwhelmingly positive in all seasons, strong in the spring and summer and especially
413 strong in the southwest. These reflect warming trends. In contrast the trends in actual
414 vapor pressure, e_a , are not uniformly positive. e_a has been rising in the southeast in fall,
415 in the south central U.S. in winter, across the whole eastern U.S. in spring and the whole
416 eastern U.S. plus northern Plains in summer. However, e_a has actually been falling in the
417 southwest in summer, as noted before by Isaac and van Wijngaarden (2012) using station
418 data from 1948 to 2010. As a consequence of the rise in e_s and drop in e_a there has been

419 a strong trend to increased VPD in the southwest in spring and summer. Elsewhere in the
420 west in summer VPD has also increased due to the rise in e_s . In the northern Plains (and
421 to a lesser extent across the north U.S.) VPD has actually decreased as e_a has risen but e_s
422 (and hence temperature) has stayed steady. These trends in the West are consistent with
423 identified trends in wildfires (Dennison et al. 2014).

424 **9. Changes in VPD up to and during the June 2002**

425 **Hayman and Rodeo-Chediski fires**

426 As mentioned in the Introduction, a main motivation of this paper is the previously
427 demonstrated importance of VPD to the occurrence of forest fires in the western U.S. Two
428 important fires of the past decade are the Rodeo-Chediski fire in Arizona and the Hayman
429 fire in Colorado, both of which began in June 2002, in the heart of a major multiyear western
430 drought (Seager 2007; Weiss et al. 2009; Cayan et al. 2010). The Rodeo-Chediski fire burned
431 from June 18 to July 7 2002 and burned 189,095 hectares of ponderosa pine and mixed
432 conifers in northern Arizona, worse than any previous recorded Arizona fire (Schoennagel
433 et al. 2004). The Hayman fire was smaller and burned 55,915 hectares to the southwest
434 of Denver beginning on June 9 2002 (Schoennagel et al. 2004) and remains the worst fire
435 in recorded Colorado history. Further, based on dendroecological records Williams et al.
436 (2013) found 2002 to be the most severe year for forest drought stress in the Southwest since
437 at least 1000 C.E. These facts motivate the presentation here of meteorological conditions
438 and VPD anomalies in the months preceding the June 2002 fires.

439 Figure 9 shows conditions during the previous winter, JFM 2002, in terms of standardized
440 anomalies. Very high VPD was evident across the southwest in JFM 2002 with maximum
441 values in Arizona but not widespread in Colorado. Precipitation was below climatological
442 normal across almost all of western North America. The Bowen ratio was high in the interior
443 southwest in Arizona, New Mexico and Colorado consistent with a drier than normal land
444 surface. Subsidence was also widespread across western North America occurring within
445 northwesterly flow. All of these prior winter conditions are conducive to elevating fire risk

446 with both land surface and atmospheric drying being responsible. Figure 10 shows the same
447 conditions for AMJ 2002. By spring high VPD anomalies had spread across the western U.S.
448 centered on Arizona, New Mexico, Utah and Colorado, reaching three standard deviations
449 in most locations. Precipitation was also below normal by two or more standard deviations
450 across the western U.S. and the Bowen ratio was elevated by two or more standard deviations
451 across the southwest. Unlike in the previous season, a southwesterly flow anomaly was
452 associated with anomalous ascent. The precipitation, land surface conditions and VPD state
453 remained conducive to elevated fire risk as in the previous season. These relations, within
454 the context of two specific historic fires, support the idea of VPD exerting an influence on
455 fire and also the influence of contemporary and prior atmosphere and land surface conditions
456 on the VPD .

457 10. Conclusions

458 To our knowledge this is the first comprehensive study of vapor pressure deficit (VPD)
459 which was recommended by Anderson (1936) as a more useful measure of the moisture
460 state of the atmosphere than relative humidity (RH). Unlike RH , for which the same value
461 can be associated with very different moisture conditions depending on the air temperature,
462 VPD is an absolute measure of the moisture deficit of the atmosphere. Hence, VPD , is
463 more closely related to the water stress on vegetation. Indeed, prior work has shown the
464 relationship between VPD variability and burned forest area in the southwest U.S (Williams
465 et al. 2014b). That relation is the prime motivation for this study since it makes clear that
466 a better understanding of the climatology, variability and trends of VPD is needed.

467 • VPD follows a notable seasonal cycle with minimum values in the winter and maximum
468 values in the summer. This is controlled by both the seasonal cycles of temperature
469 and humidity. Because of the development of the subtropical anticyclones, which
470 moisten the eastern U.S. and dry the western U.S., actual vapor pressure has a summer
471 maximum in the southeast but remains low in the west. In contrast, saturation vapor
472 pressure in summer maximizes in the interior southwest, southern and central Plains
473 and the southeast. Combining these influences, VPD in summer is far greater in the

474 west than in the east. VPD reaches its all-U.S. maximum in summer at the California-
475 Arizona border but more general maxima extend across the southwest U.S.

- 476 • The variance of VPD has a minimum in fall and then strengthens into winter and
477 then to spring and to summer. The southwest and the southern Plains stand out as
478 maxima of variance in spring and summer. The VPD variance quite closely tracks the
479 saturation vapor pressure variance but the southwest and the southern Plains are also
480 regions of relatively strong variance of actual vapor pressure. Hence it appears that
481 VPD variability can be influenced by both thermodynamic and dynamic processes.
- 482 • High VPD in the interior southwest U.S. is associated with La Niña conditions in
483 the tropical Pacific Ocean in fall, winter and spring. This association works via ocean
484 forcing of circulation anomalies that involve high pressure and northerly, subsiding
485 flow over the southwest. Such flow warms, increasing saturation vapor pressure, and
486 dries, decreasing actual vapor pressure, and, hence, causes VPD to increase. Summer
487 VPD anomalies in the southwest are controlled by more local circulation anomalies
488 that influence saturation vapor pressure.
- 489 • High VPD in spring and summer can also be caused by an increase in Bowen ratio,
490 that is an increase in sensible heat flux relative to latent heat flux, although the causes
491 of this are distinct in the eastern and western U.S. In the western U.S. low surface
492 moisture, following a drop in precipitation for example, can cause an increase in Bowen
493 ratio and VPD .
- 494 • A case study of conditions in advance of the June 2002 Rodeo-Chediski and Hayman
495 fires in Arizona and Colorado, respectively, shows very high VPD that was caused
496 by precipitation drops, an increase in Bowen ratio and anomalous subsidence in the
497 preceding months. This reveals the complexity of meteorological processes that can
498 increase drying of the land surface and vegetation and set the stage for serious fires.
- 499 • Since 1961 VPD has increased notably across the western U.S. with the strongest
500 increases in the southwest. These trends have been primarily driven by warming that
501 increases the saturation vapor pressure but have also been contributed to by a decrease

502 in actual vapor pressure. Actual vapor pressure has increased elsewhere in the U.S.
503 such that VPD has declined in the northern Plains and midwest.

504 This is the first comprehensive study of vapor pressure deficit since Anderson (1936)
505 argued for its use instead of relative humidity as a measure of the moisture state of the
506 atmosphere. As an absolute measure of the difference between actual and potential water
507 vapor holding capacity of the atmosphere, VPD is a useful indicator of the ability of the
508 atmosphere to extract moisture from the land surface and, hence, is of relevance in studies of
509 the links between meteorological conditions and forest fires. Here we have sought to achieve
510 a basic understanding of the climatology and variability of VPD across the United States
511 and have explained these in terms of atmospheric and land surface conditions. Future work
512 will investigate closely the links between fires and VPD variability and the surface and
513 atmospheric conditions that control them.

514 *Acknowledgments.*

515 This work was supported by NSF award AGS-1243204 (Linking Near-term Future Changes
516 in Weather and Hydroclimate in Western North America to Adaptation for Ecosystem and
517 Water Management). AH was supported by an Earth Institute at Columbia University un-
518 dergraduate research internship. The GLDAS data used in this study were acquired as part
519 of the NASA's Earth-Sun System Division and archived and distributed by the Goddard
520 Earth Sciences (GES) Data and Information Services Center (DISC) Distributed Active
521 Archive Center (DAAC). LDEO Contribution Number XXXX.

REFERENCES

- 524 Abatzoglou, J. T. and C. A. Kolden, 2013: Relationships between climate and macroscale
525 area burned in the western United States. *Int. J. Wildland Fire*, **22**, 1003–1020.
- 526 Adams, D. and A. Comrie, 1997: The North American monsoon. *Bull. Amer. Meteor. Soc.*,
527 **78**, 2197–2213.
- 528 Allen, C. D., et al., 2010: A global overview of drought and heat-induced tree mortality
529 reveals emerging climate change risks for forests. *Forest Ecol. Manag.*, **259**, 660–684.
- 530 Anderson, D. B., 1936: Relative humidity or vapor pressure deficit. *Ecology*, **17**, 277–282.
- 531 Bentz, B. J., et al., 2010: Climate change and bark beetles of the western United States and
532 Canada: Direct and indirect effects. *BioScience*, **60**, 602–613.
- 533 Cayan, D., T. Das, D. Pierce, T. Barnett, M. Tyree, and A. Gershunov, 2010: Future dryness
534 in the southwest United States and the hydrology of the early 21st Century drought. *Proc.*
535 *Nat. Acad. Sci.*, **107**, 21 271–21 276.
- 536 Daly, C., W. P. Gibson, G. H. Taylor, G. L. Johnson, and P. Pasteris, 2000: High quality
537 spatial climate data sets for the United States and beyond. *Trans. Am. Soc. Ag. Eng.*, **43**,
538 1957–1962.
- 539 Dennison, P. E., S. C. Brewer, J. D. Arnold, and M. A. Moritz, 2014: Large wildfire trends
540 in the western United States, 1984–2011. *Geophys. Res. Lett.*, doi:10.1002/2014GL059576.
- 541 Eidenshink, J., B. Schwind, K. Brewer, Z.-L. Zhu, B. Quayle, and S. Howard, 2007: A
542 project for monitoring trends in burn severity. *Fire Ecol.*, **3**, 3–21.
- 543 Gaffen, D. J. and R. J. Ross, 1999: Climatology and trends of U.S. surface humidity and
544 temperature. *J. Climate*, **12**, 811–828.

545 Isaac, V. and W. A. van Wijngaarden, 2012: Surface water vapor pressure and temperature
546 trends in North America during 1948-2010. *J. Climate*, **25**, 3599–3609.

547 Kalnay, E. et al., 1996: The NCEP/NCAR 40-year reanalysis project. *Bull. Am. Meteor.*
548 *Soc.*, **77**, 437–471.

549 Kistler, R., et al., 2001: The NCEP-NCAR 50-year Reanalysis: Monthly means CD-ROM
550 and documentation. *Bull. Am. Meteor. Soc.*, **82**, 247–268.

551 Kumar, A. and M. P. Hoerling, 1998: Annual cycle of Pacific-North American seasonal
552 predictability associated with different phases of ENSO. *J. Climate*, **11**, 3295–3308.

553 Littell, J. S., D. McKenzie, D. L. Peterson, and A. L. Westerling, 2009: Climate and wildfire
554 area burned in Western US ecoregions, 1916-2003. *Ecol. Applications*, **19**, 1003–1021.

555 Pyne, S. J., 2009: Fire on the fringe. *Env. Res. Lett.*, **4**, 031004.

556 Riley, K. L., J. T. Abatzoglou, I. C. Grenfell, A. E. Klene, and F. A. Heinsch, 2013: The
557 relationship of large fire occurrence with drought and fire danger indices in the western
558 USA, 1984-2008: the role of temporal scale. *Int. J. Wildland Fire*, **22**, 894–909.

559 Rodell, M., et al., 2004: The Global Land Data Assimilation System. *Bull. Amer. Meteor.*
560 *Soc.*, **85**, 381–394.

561 Schoennagel, T., T. T. Veblen, and W. H. Rome, 2004: The interaction of fire, fuels and
562 climate across Rocky Mountain forest. *Bioscience*, **54**, 661–676.

563 Seager, R., 2007: The turn-of-the-century North American drought: dynamics, global con-
564 text and prior analogues. *J. Climate*, **20**, 5527–5552.

565 Seager, R., L. Goddard, J. Nakamura, N. Naik, and D. Lee, 2014a: Dynamical causes of the
566 2010/11 Texas-northern Mexico drought. *J. Hydromet.*, **15**, 39–68.

567 Seager, R., N. Harnik, Y. Kushnir, W. Robinson, and J. Miller, 2003a: Mechanisms of
568 hemispherically symmetric climate variability. *J. Climate*, **16**, 2960–2978.

569 Seager, R., N. Harnik, W. A. Robinson, Y. Kushnir, M. Ting, H. P. Huang, and J. Velez,
570 2005: Mechanisms of ENSO-forcing of hemispherically symmetric precipitation variability.
571 *Quart. J. Roy. Meteor. Soc.*, **131**, 1501–1527.

572 Seager, R., R. Murtugudde, N. Naik, A. Clement, N. Gordon, and J. Miller, 2003b: Air-
573 sea interaction and the seasonal cycle of the subtropical anticyclones. *J. Climate*, **16**,
574 1948–1966.

575 Seager, R., D. Neelin, I. Simpson, H. Liu, N. Henderson, T. Shaw, Y. Kushnir, and M. Ting,
576 2014b: Dynamical and thermodynamical causes of large-scale changes in the hydrological
577 cycle over North America in response to global warming. *J. Climate*, in press.

578 Sedano, F. and J. T. Randerson, 2014: Vapor pressure deficit controls on fire ignition and
579 fire spread in boreal forest ecosystems. *Biogeosciences Discussions*, **11**, 1309–1353.

580 Sheffield, J. and G. G. E. Wood, 2006: Development of a 50-yr high-resolution global dataset
581 of meteorological forcings for land surface modeling. *J. Climate*, **19**, 3088–3111.

582 Stephens, S. L., J. K. Agee, P. Z. Fule, M. P. North, W. H. Romme, T. W. Swetnam, and
583 M. G. Turner, 2013: Managing forests and fire in changing climates. *Science*, **342**, 41–42.

584 Swetnam, T. W. and J. L. Betancourt, 1998: Mesoscale disturbance and ecological response
585 to decadal climate variability in the American southwest. *J. Climate*, **11**, 3128–3147.

586 Weiss, J. L., C. L. Castro, and J. T. Overpeck, 2009: Distinguishing pronounced droughts
587 in the southwestern United States: Seasonality and effects of warmer temperatures. *J.*
588 *Climate*, **22**, 5918–5932.

589 Westerling, A. L. and B. P. Bryant, 2008: Climate change and wildfire in California. *Clim.*
590 *Change*, **87**, S231–S249.

591 Westerling, A. L., A. Gershunov, T. J. Brown, D. R. Cayan, and M. D. Dettinger, 2003:
592 Climate and wildfire in the western United States. *Bull. Amer. Meteor. Soc.*, **84**, 595–604.

- 593 Westerling, A. L., A. Gershunov, D. R. Cayan, and T. P. Barnett, 2002: Long lead statistical
594 forecasts of area burned in western US wildfires by ecosystem province. *Int. J. Wildland*
595 *Fire*, **11**, 257–266.
- 596 Westerling, A. L., H. G. Hidalgo, , D. R. Cayan, and T. W. Swetnam, 2006: Warming and
597 earlier spring increase western US forest wildfire activity. *Science*, **313**, 940–943.
- 598 Williams, A. P., et al., 2013: Temperature as a potent driver of regional forest drought stress
599 and tree mortality. *Nature Climate Change*, **3**, 292–297.
- 600 Williams, A. P., et al., 2014a: Causes and future implications of extreme 2011 atmospheric
601 moisture demand and wildfire in the southwest United States. *J. Appl. Meteor. Climate*,
602 submitted.
- 603 Williams, A. P., et al., 2014b: Correlations between components of the water balance and
604 burned area reveal new insights for predicting forest-fire area in the southwest United
605 States. *Int. J. Wildland Fire*, submitted (revised May 2014).

606 List of Figures

- 607 1 The climatology of vapor pressure deficit VPD (left), saturation vapor pres-
608 sure e_s (middle) and actual vapor pressure e_a (right) for the October to
609 November (fall, top), December to February (winter, upper middle), March
610 to May (spring, lower middle) and June to July (summer, bottom) seasons.
611 Units are hPa (or mb). 26
- 612 2 Same as Figure 1 but for variances. Units are hPa squared. 27
- 613 3 Same as Figure 2 but with the variances divided by the climatological values. 28
- 614 4 Areas burned over 1984 to 2011 marked as brown on top of forest areas marked
615 as green. Data from the Monitoring Trends in Burn Severity program. 29
- 616 5 The correlations between VPD (left), e_s (middle) and e_a (right) in the U.S.
617 Southwest and 700hPa geopotential heights (contours) and SST (colors) anoma-
618 lies for fall (top), winter (upper middle), spring (lower middle) and summer
619 (bottom). 30
- 620 6 The correlations between Bowen ration and VPD (left), e_s (middle) and e_a
621 (right) for fall (top), winter (upper middle), spring (lower middle) and summer
622 (bottom). 31
- 623 7 The actual VPD for AMJ and its reconstruction via linear regression based
624 on AMJ Bowen ratio alone (V_b) and both AMJ Bowen ratio and AMJ 700mb
625 geopotential height (V_{bh}). 32
- 626 8 Linear trends in VPD , e_s and e_a for 1960 to 2012 for fall (top), winter (upper
627 middle), spring (lower middle) and summer (bottom). Units are hPa change
628 over the 53 year period. 33
- 629 9 Conditions in the winter before the Rodeo-Chediski and Hayman fires of June
630 2002. Shown for JFM 2002 are the standardized anomalies of VPD (upper
631 left), precipitation (upper right), Bowen ratio (lower left) and 700mb vertical
632 velocity (colors) and geopotential heights (contours) (bottom right). 34

Climatology of Vapor Pressure (VP)

VP Difference (left), Saturation VP (middle), Actual VP (right)

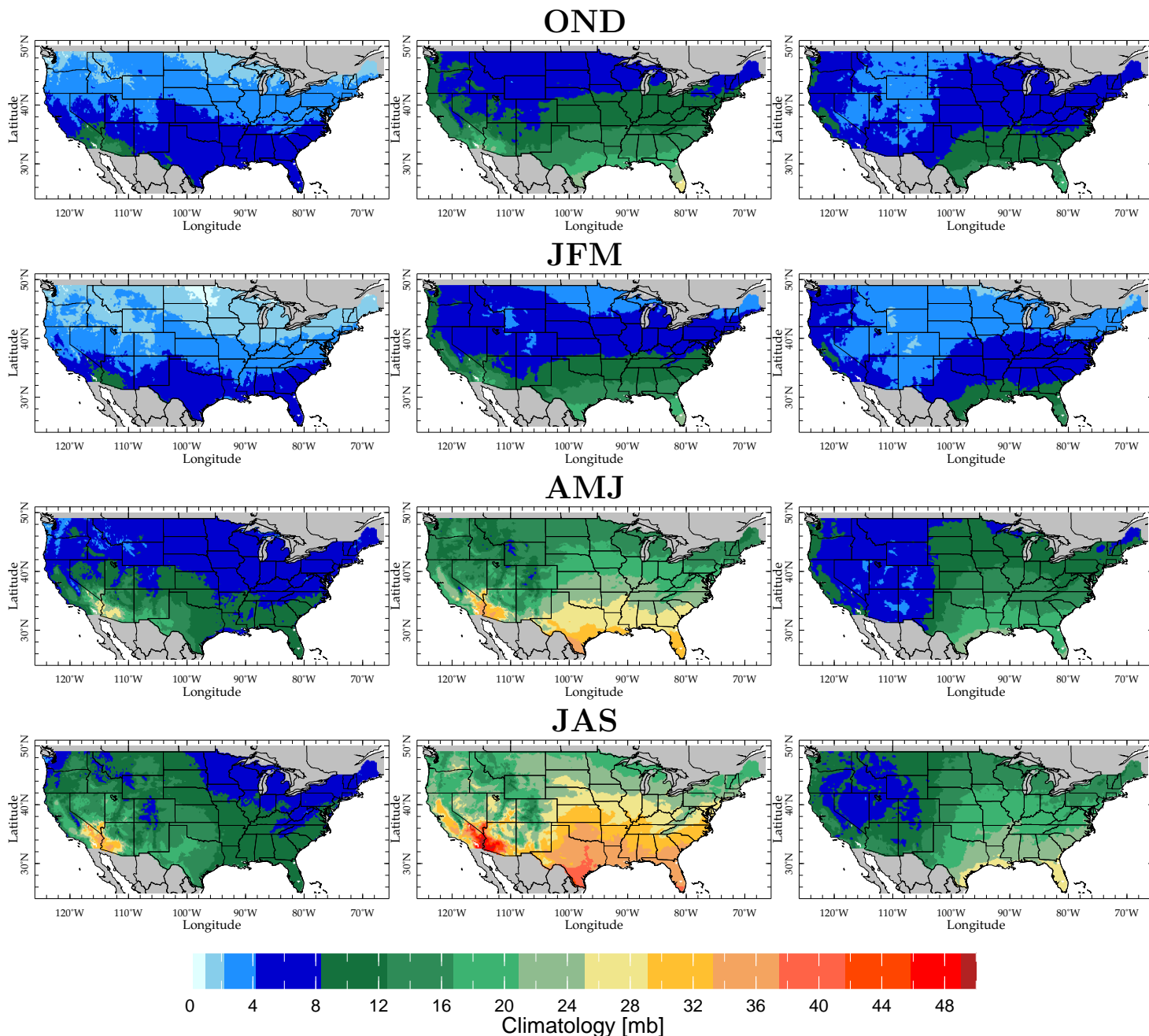


FIG. 1. The climatology of vapor pressure deficit VPD (left), saturation vapor pressure e_s (middle) and actual vapor pressure e_a (right) for the October to November (fall, top), December to February (winter, upper middle), March to May (spring, lower middle) and June to July (summer, bottom) seasons. Units are hPa (or mb).

Variance of Vapor Pressure (VP)

VP Difference (left), Saturation VP (middle), Actual VP (right)

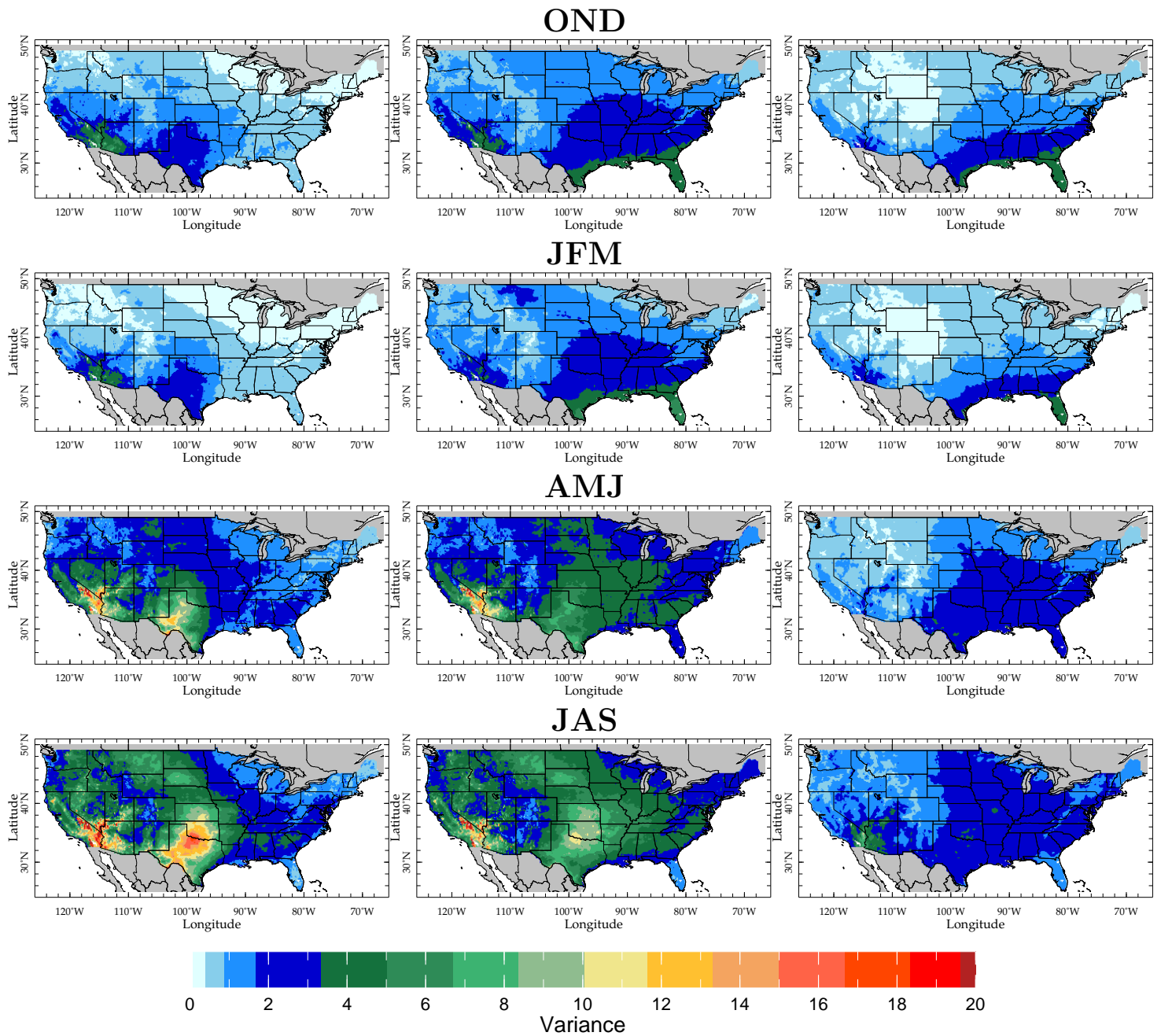


FIG. 2. Same as Figure 1 but for variances. Units are hPa squared.

Variance/Climatology of Vapor Pressure (VP)

VP Difference (left), Saturation VP (middle), Actual VP (right)

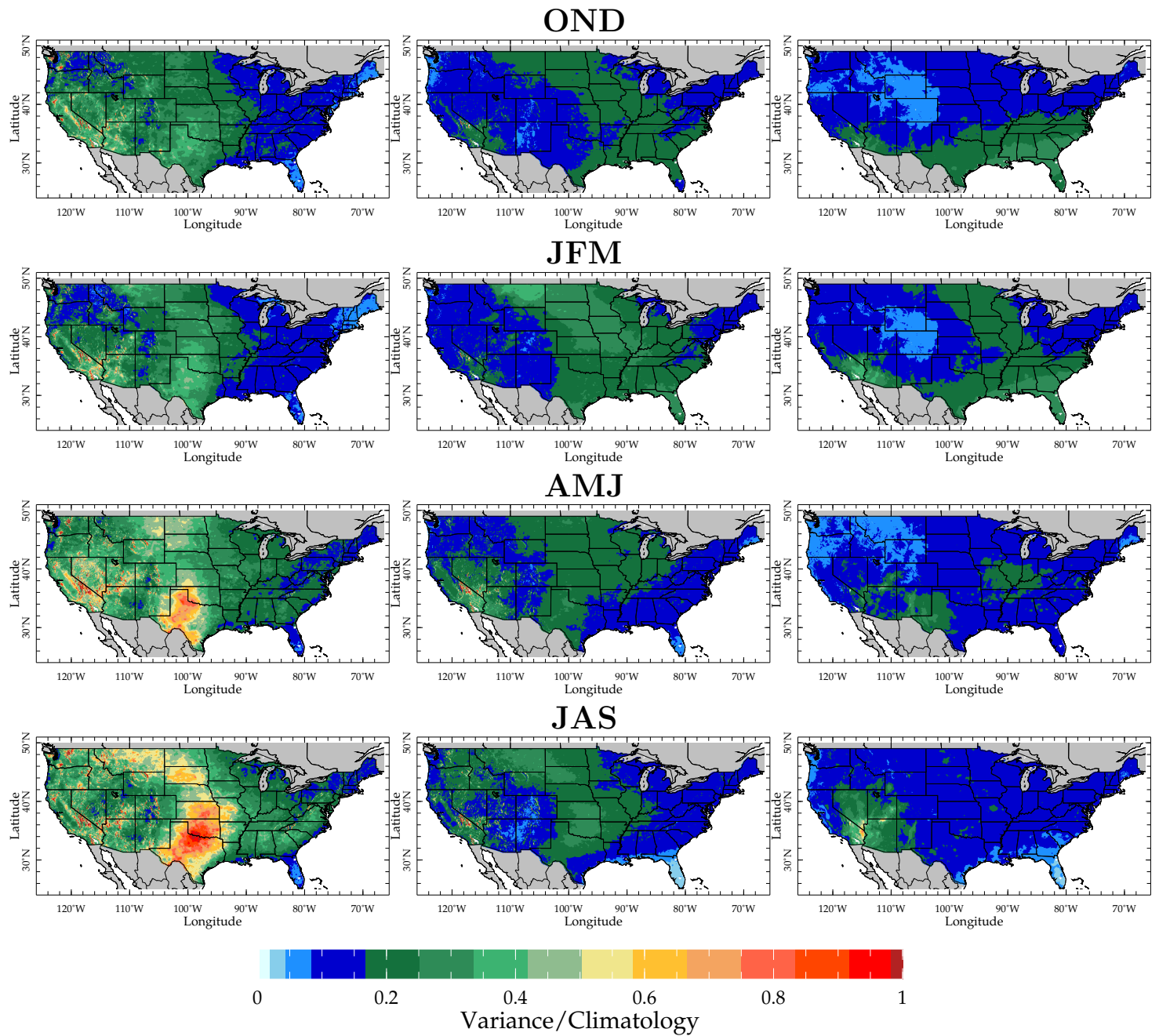


FIG. 3. Same as Figure 2 but with the variances divided by the climatological values.

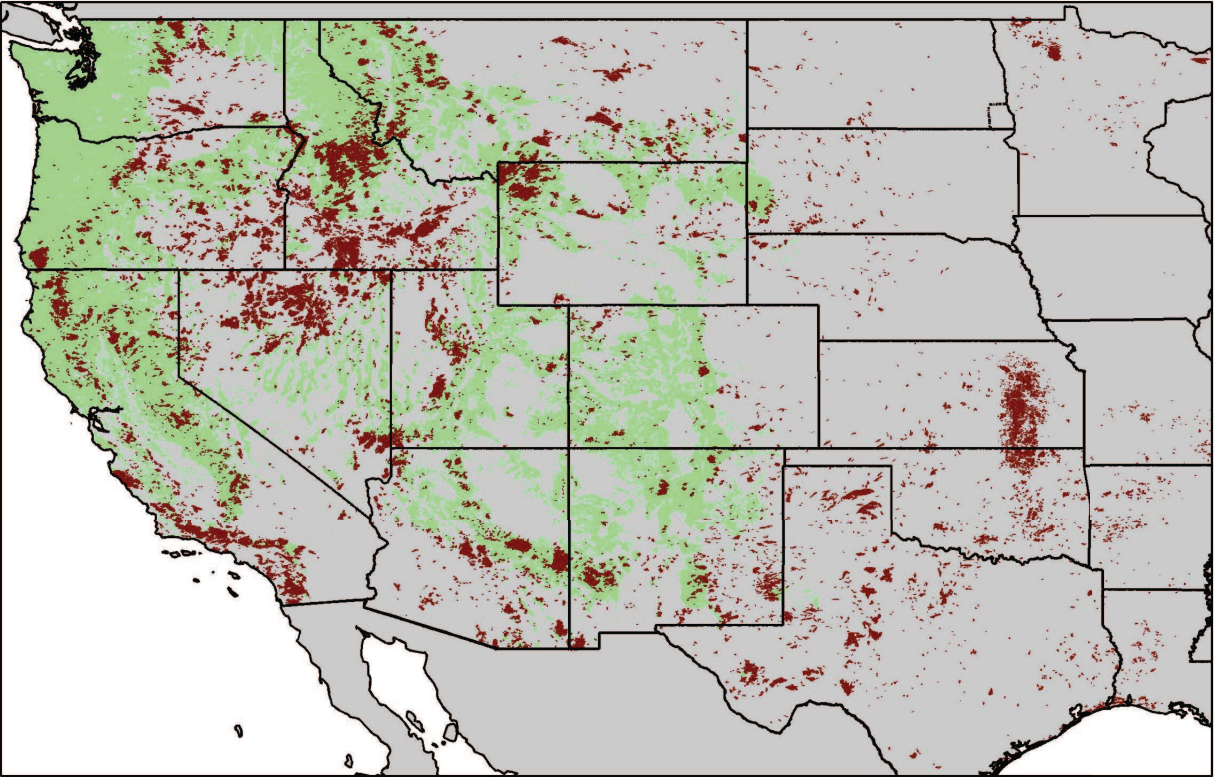


FIG. 4. Areas burned over 1984 to 2011 marked as brown on top of forest areas marked as green. Data from the Monitoring Trends in Burn Severity program.

Correlation of Vapor Pressure (VP) on SSTA (colors), 700 mb Heights (contours)
 VP Difference (left), Saturation VP (middle), Actual VP (right)

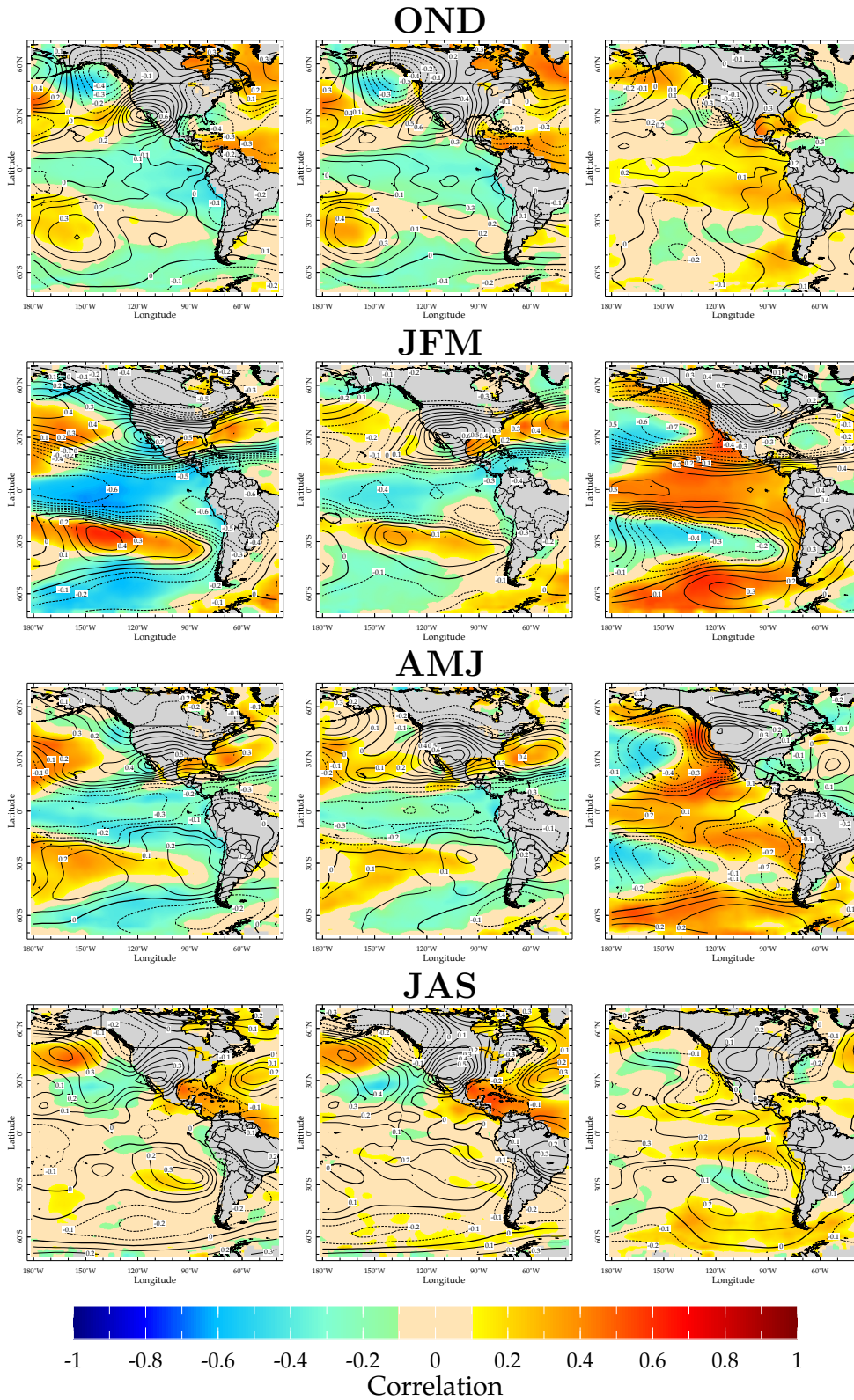


FIG. 5. The correlations between VPD (left), e_s (middle) and e_a (right) in the U.S. Southwest and 700hPa geopotential heights (contours) and SST (colors) anomalies for fall (top), winter (upper middle), spring (lower middle) and summer (bottom).

Correlation of Bowen Ratio with Vapor Pressure (VP)

VP Difference (left), Saturation VP (middle), Actual VP (right)

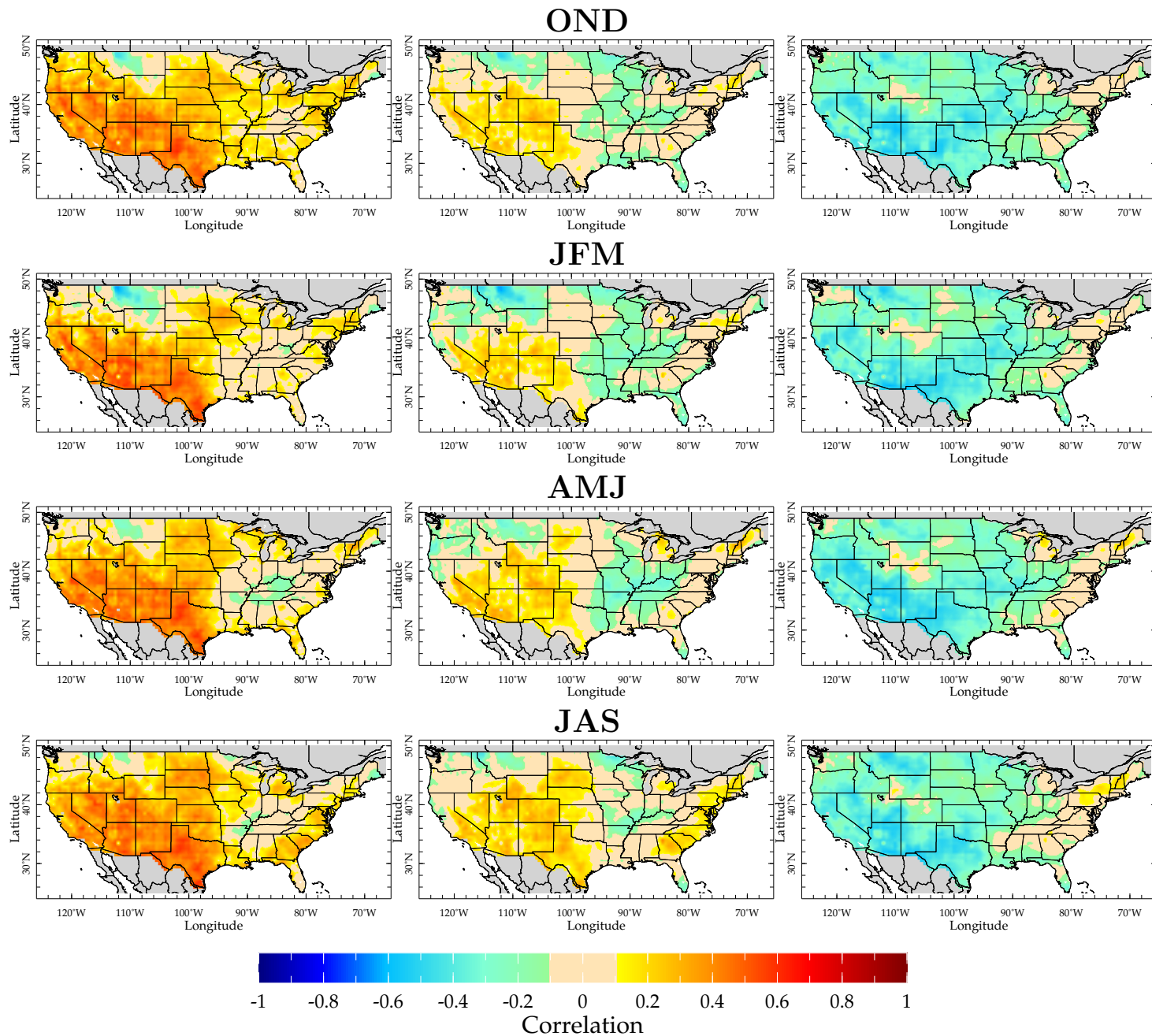
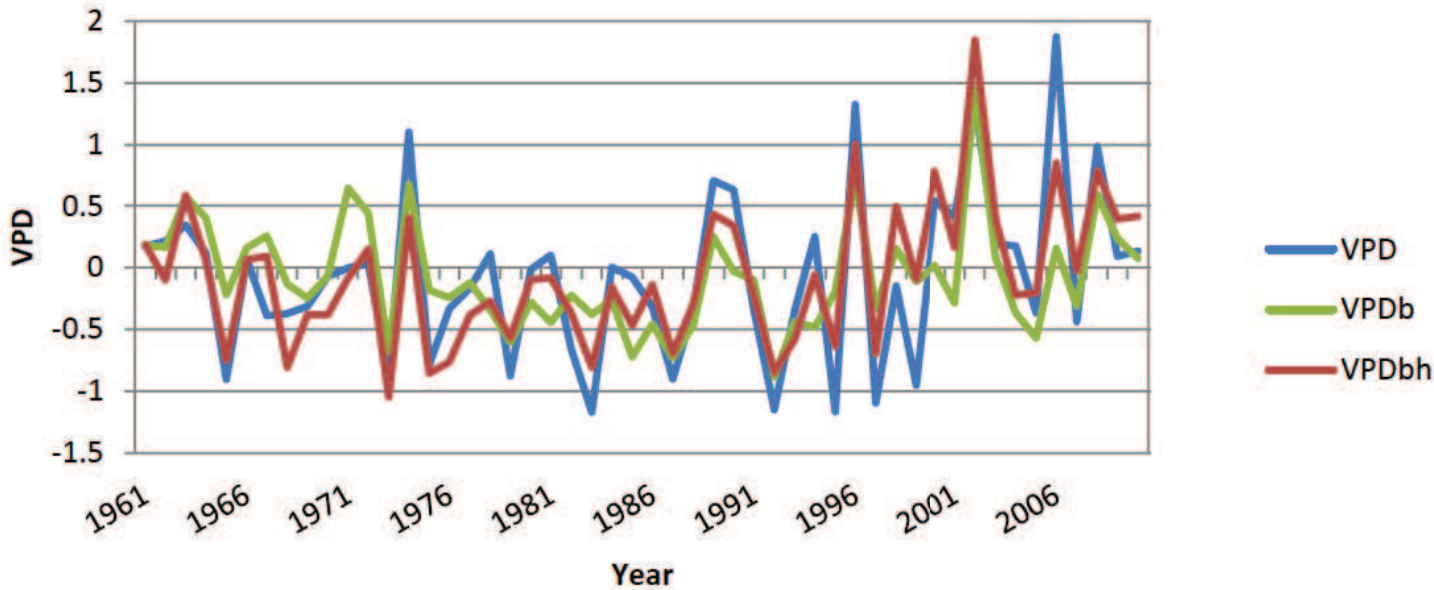


FIG. 6. The correlations between Bowen ratio and VPD (left), e_s (middle) and e_a (right) for fall (top), winter (upper middle), spring (lower middle) and summer (bottom).

AMJ Standardized VPD for SW Area



AMJ Standardized VPD for Colorado Area

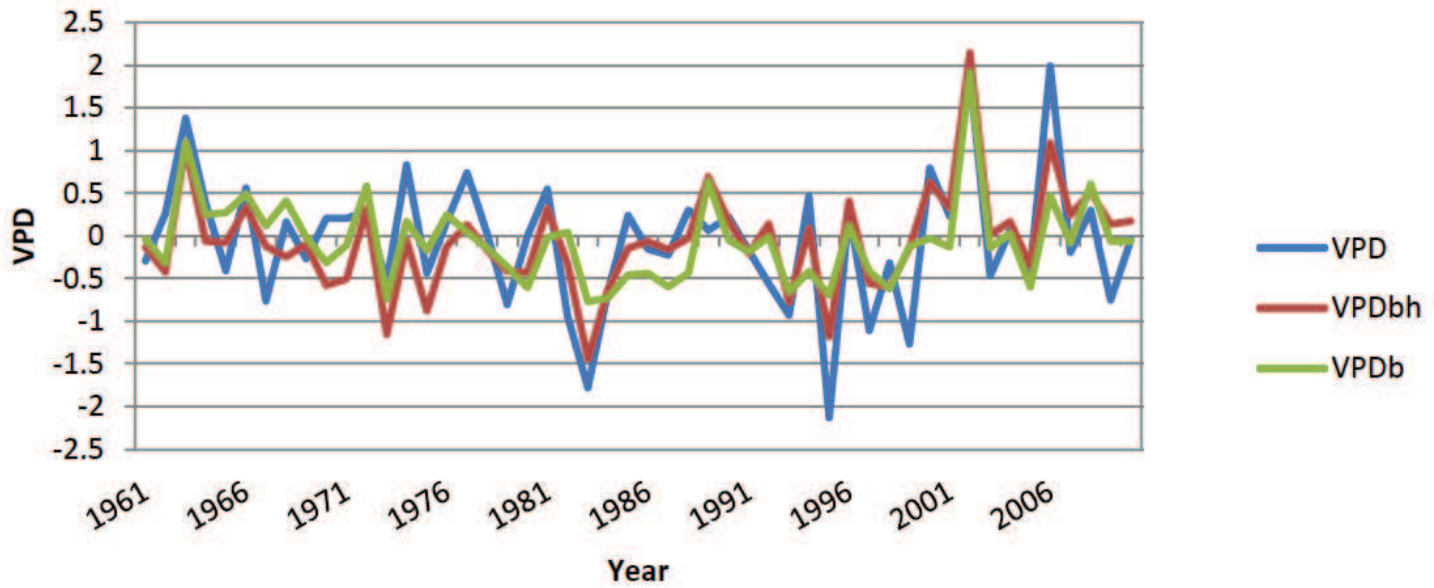


FIG. 7. The actual VPD for AMJ and its reconstruction via linear regression based on AMJ Bowen ratio alone (V_b) and both AMJ Bowen ratio and AMJ 700mb geopotential height (V_{bh}).

Trend of Vapor Pressure (VP) 1961-2012/2013

VP Difference (left), Saturation VP (middle), Actual VP (right)

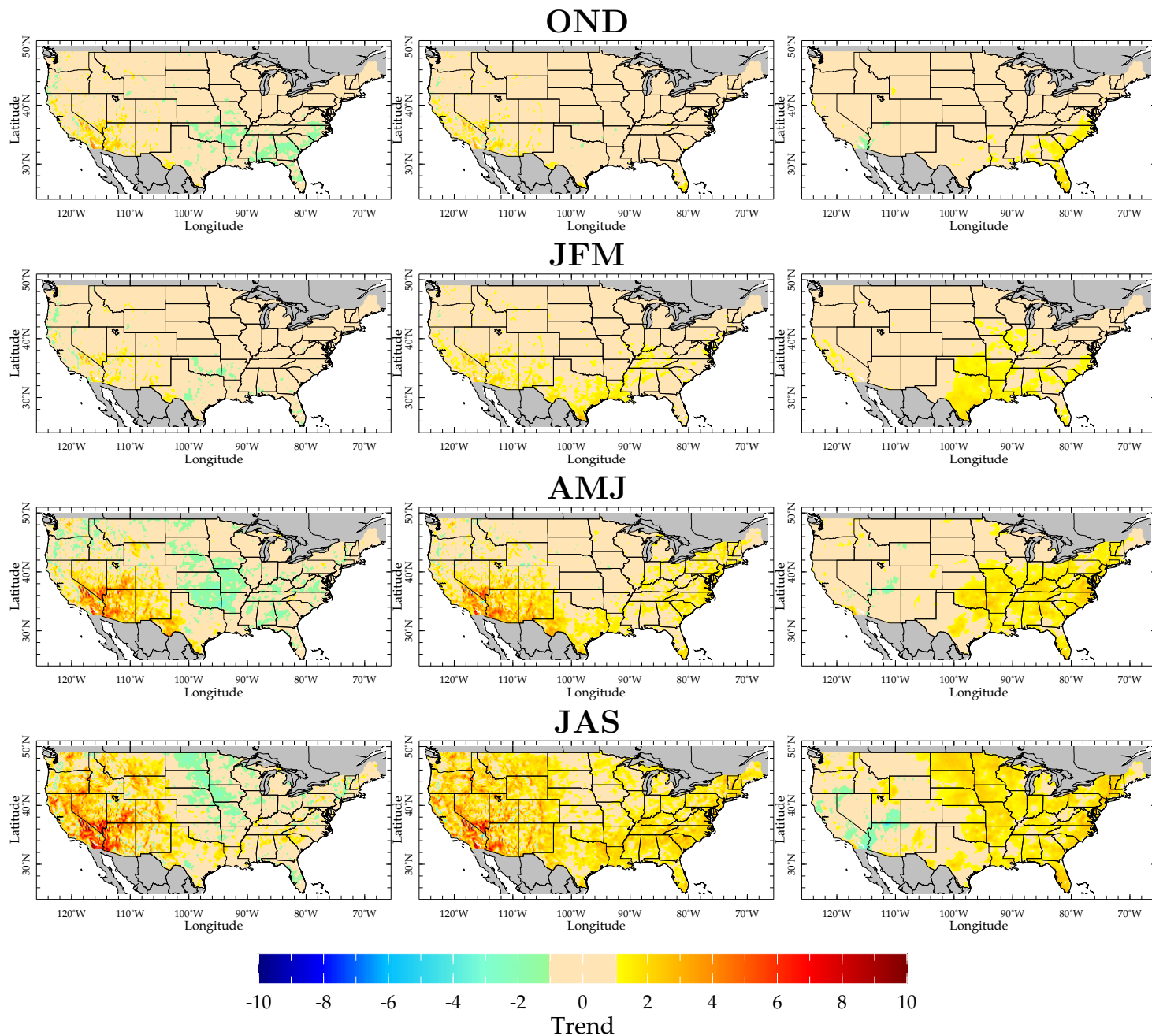


FIG. 8. Linear trends in VPD , e_s and e_a for 1960 to 2012 for fall (top), winter (upper middle), spring (lower middle) and summer (bottom). Units are hPa change over the 53 year period.

JFM 2002

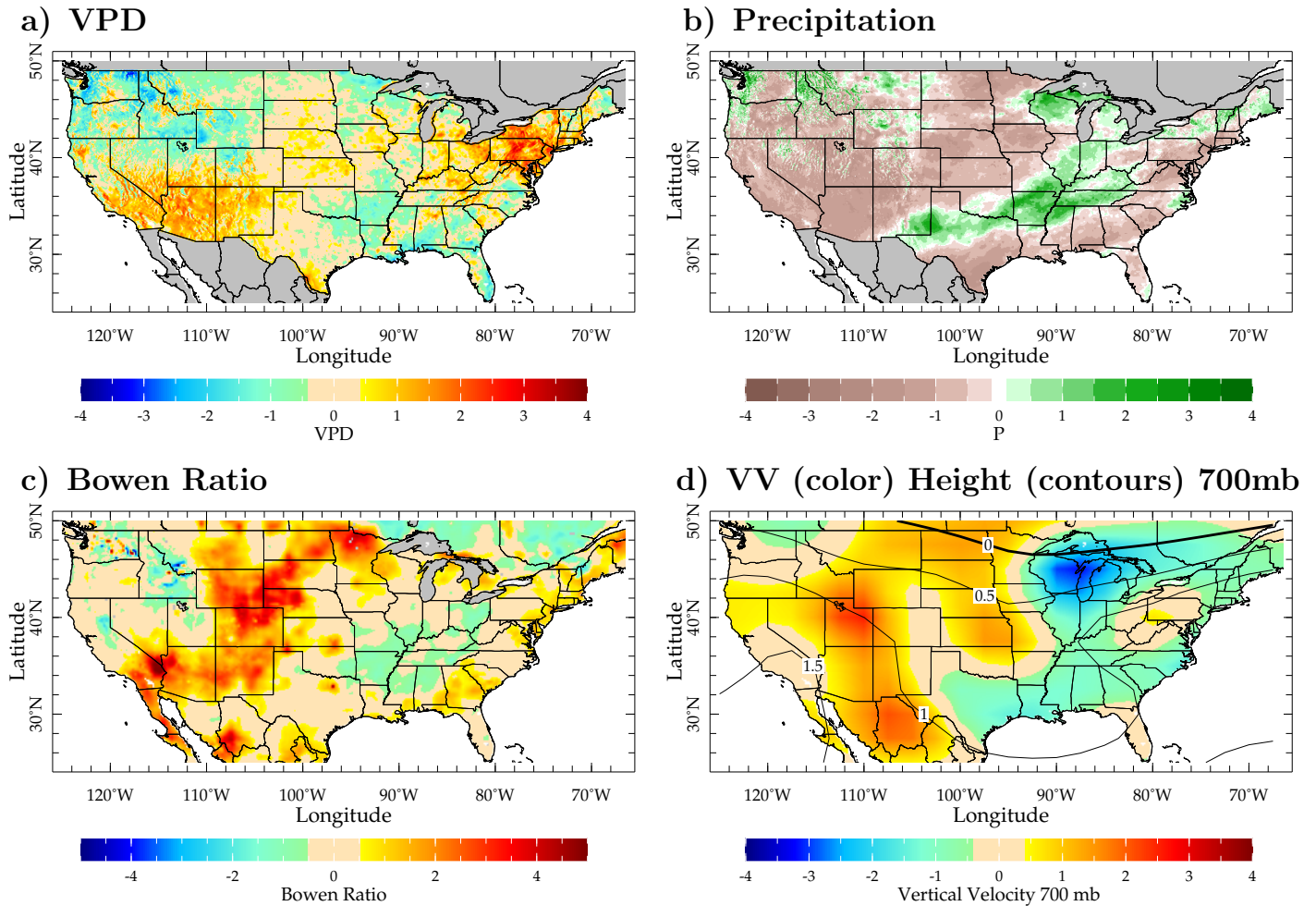


FIG. 9. Conditions in the winter before the Rodeo-Chediski and Hayman fires of June 2002. Shown for JFM 2002 are the standardized anomalies of VPD (upper left), precipitation (upper right), Bowen ratio (lower left) and 700mb vertical velocity (colors) and geopotential heights (contours) (bottom right).

AMJ 2002

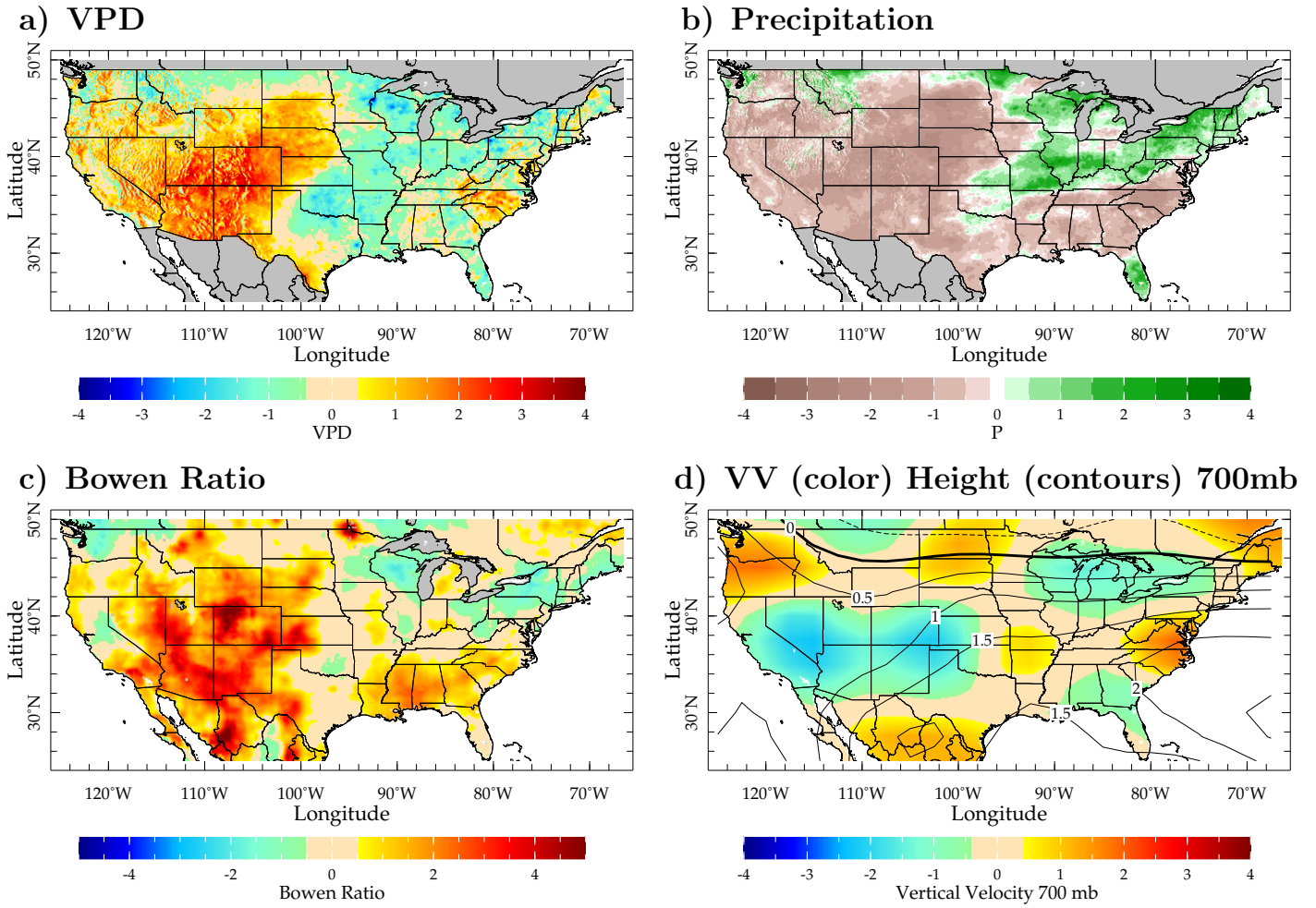


FIG. 10. Same as Figure 9 but for AMJ 2002.